https://doi.org/10.1016/j.jmbbm.2019.05.030

Title: The effect of ethanol on surface of semi-interpenetrating polymer network (IPN) polymer matrix of glass-fibre reinforced composite.

Abstract

Aim of the study: The aim of this laboratory study was to evaluate the effect of ethanol treatment on the surface roughness (S_a), nano-mechanical properties (NMP) and chemical characterization of dental fiber reinforced composite (FRC) with semi-interpenetrating polymer network (IPN).

Materials and Methods: A total of 240 FRC specimens with bisphenol A-glycidyl methacrylate - triethyleneglycol dimethacrylate – Poly (methylmetahcrylate) (*bis*-GMA-TEGDMA-PMMA) IPN matrix system were light cured for 40 s and divided into 2 groups (L and LH). The group LH was further post-cured by heat at 95°C for 25 min. The specimens were exposed to 99.9%, 70% and 40% for 15, 30, 60 and 120 s respectively. The treated specimens were evaluated for surface roughness using non-contact profilometer. Nano-mechanical properties were determined using nanoindentation technique and chemical characterization was assessed by Fourier Transform-Infrared (FTIR) spectroscopic analyses. Scanning electron microscopic (SEM) images were made to evaluate the surface topographical changes.

Results: Both the L and LH group showed changes in the S_a and NMP after being treated by different concentrations of ethanol and at different time interval. The highest S_a was observed with L-group (0.733 μm) treated with 99.9 % ethanol for 120 s. Specimens in LH-group treated with 99.9 % ethanol for 120 s (1.91GPa) demonstrated increased nano-hardness, and group treated with 40 % ethanol for 120 s demonstrated increased Young's modulus of elasticity

(22.90 GPa). FTIR analyses revealed changes in the intensity and band width in both the L and LH groups.

Conclusion: The present study demonstrated that both light-cured and heat post-cured FRC were prone for ethanol induced alteration in the surface roughness (S_a), nano-mechanical properties (NMP) and chemical characterization. The interphase between the glass fibers and the organic matrix was affected by ethanol. The changes were considerably less in magnitude in the heat post-cured FRC specimens.

Key words: Ethanol, Dissolution, Solvents, FRC, Interpenetrating polymer network,

1. Introduction

Modern dentistry includes various materials such as polymers and composites for restoring and reconstruction of teeth and replacing missing teeth. Earlier in 1860's natural rubber and synthetic polymers were used as denture base polymers until the introduction of poly (methyl methacrylate) in the late 1930's (Sweeney and Caul, 1940). Introduction of cross-linking thermoset monomers by Bowen (Bowen, 1963) such as dimethacrylate monomers paved the way for the use of interpenetrating polymer networks (IPN)-like structures in the field of dentistry. Present day, the IPN-like structures are found in denture teeth, fibre-reinforced composites (FRC), denture base polymers and restorative resin composite materials (Garoushi et al., 2008; Vallittu, 2009). IPNs are considered as unique "alloys" of cross-linked polymers (Nowers and Narasimhan, 2006) formed by a combination of two or more polymers in a network form synthesized in juxtaposition (Sperling, 1994). Aylsworth was the pioneer to use the concept of IPNs. He combined the phenol-formaldehyde composition with natural rubber and sulphur and the science of IPNs began with the work of Millar in the early 1960's (Sperling, 1985). IPNs are also defined as polymer networks that are entangled by topological interactions, wherein the inter-network entanglements are permanent as they are chemically cross-linked (Klempner et al., 1970). This chemical cross-linking makes the material difficult to be "pulled apart" without fracturing either of the polymer networks (Myung et al., 2008). The significant property of dental IPN structures is their ability of partial dissolution of their surface, which makes the surface useful for adhering new resin systems to the IPN polymer or IPN polymer matrix resin composite (Bell et al., 2005; Lastumäki et al., 2002; Wolff et al., 2012)

Fibre-reinforced composites (FRC) have been developed to a variety of dental disciplines and applications: removable prosthodontics, restorative dentistry, periodontology, orthodontics along with repair of fractured porcelain veneers (Kolbeck et al., 2002). An FRC is a combination of reinforced fibres in a polymer matrix. Silanized glass fibres (Matinlinna et al., 2004; Matinlinna et al., 2018) are reinforcing dental polymers and it is widely documented that glass fibres are superior to carbon carbon and aramid fibres for their reinforcing efficiency and aesthetic qualities (Vallittu, 1996). The factors that govern the efficacy of fibres reinforced depend on the resins used, quantity, length (Vallittu et al., 1994), form (Ladizesky et al., 1993), orientation (Dyer et al., 2004), adhesion of fibres to the polymer matrix, and impregnation of fibres within the resin (Miettinen and Vallittu, 1997; Vallittu, 1994, 1995). The reinforced fibres could be continuous (unidirectional or bidirectional), or random that are continuous or discontinuous (short). Selection of the form of the fibres is based on the clinical application. For example in root anchoring systems continuous unidirectional fibres are preferred.

Dental adhesives are solvated in various organic solvents such as ethanol, acetone, *tert*-butanol, tetrahydrofuran (THF), dimethylsulfoxide (*DMSO*) and water (Ekambaram et al., 2015). Presently ethanol is the most commonly used organic hydrophilic solvent either alone or with water as a co-solvent in various commercially available dental adhesives (Reis et al., 2003). Out of the various physical properties of a solvent, vapor pressure determines the time required to evaporate from its site of application at a given temperature (Abate et al., 2000). The vapor pressure of ethanol (40 mmHg) makes it difficult to evaporate completely at an ambient temperature and atmospheric pressure. Ethanol and water forms an azeotropic mixture and increased retention of organic solvent and water has been observed (Yiu et al., 2005). It was also

found that ethanol/water containing adhesives had more impact on the durability of the resin bonding to dentine (Fontes et al., 2012). Although dental adhesives and primers are intended to be used with dentine and enamel, in certain conditions, they may be applied to the surface of resin composites as well.

Thermoplastic polymers are bound together with weak van der Waals forces between the polymer chains. Strong covalent bonds within the polymer chains are prone to solvent crazing which appears as an organized crack pattern. Solvent crazing can take place also in those areas of a polymer which have high hydrostatic tension, resulting in formation of micro-voids due to localized yielding (McLeish et al., 1989). Crazing can be seen by the reflection of light by the polymeric chain. Polymer interfiling was seen in the matrix interconnecting the polymer and was not deformed by the solvent and its width was determined by the groove formed (Basavarajappa et al., 2016). The solubility parameters of ethanol 12.92 $(cal/cm^3)^{1/2}$ and poly-(methyl methacrylate) (PMMA) 8.9-12.7 $(cal/cm^3)^{1/2}$, indicate that ethanol could potentially dissolve or craze the polymer with PMMA. Varying the concentrations of ethanol by water with a solubility parameter of 23.5 $(cal/cm^3)^{1/2}$ can potentially also alter the solubility of the surface containing PMMA (Kambour, 1973).

The semi-IPN system used in present dental FRC material is based on a cross-linked *bis*-phenol-A-glycidyldimethacrylate (*bis*-GMA), triethyleneglycol dimethacrylate (TEGDMA) and linear poly(methyl methacrylate) system. It is noteworthy that IUPAC based name for the semi IPN made of *bis*GMA, TEGDMA and PMMA is *net*-poly(methyl methacrylate)-*inter*-*net*-copoly(*bis*-glycidyl-A-dimethacrylate)-triethyleneglycol dimethacrylate (Vallittu, 2009). Recently, it was demonstrated the IPN system of dental FRC has a gradient structure regarding

the ratio of *bis*-GMA, TEGDMA and PMMA and that the concentration of the PMMA on the surface of FRC is higher than in the inner parts of the FRC (Khan et al., 2018).

Due to the composition of the IPN systems used in dental FRC and some recently published information of the influence of ethanol to the PMMA, it can be expected that ethanol of dental primers could have an influence to the polymer matrix of FRC (Basavarajappa et al., 2017; Basavarajappa et al., 2016). That said, the aim of this laboratory study was to evaluate the effect of ethanol treatment on the surface roughness (Sa), nano-mechanical properties (NMP) and chemical characterization of dental fiber reinforced composite (FRC) with semi-interpenetrating polymer network (IPN).

2. Materials and methods

2.1. Specimen Preparation

A mold made of silicone putty (Affinis Putty, Coltene/Whaledent, Altstatten, Switzerland) was used to prepare the samples and standardize their shape and size. A TOTAL OF 240 semi-IPN FRC (everStick C&B, StickTech-GC, Turku, Finland) SPECIMENS consisting of co-monomer system of *bis*-GMA-TEGDMA and PMMA.WAS PREPARED. THE SPECIMENS was cut off, AND placed inside the silicone mold, pressed against two glass plates to obtain an even and flat surface of 1mm thickness. THE FRC specimens were polymerized using a hand-held light-polymerizing unit for 40 s with an irradiance output of 1150 mW/cm2 (Elipar S10; 3M ESPE, USA). The irradiance output of the light-polymerizing unit was measured on a spectroradiometrically calibrated NIST-referenced USB 4000 spectrometer, Managing Accurate Resin Curing (MARC) device. The samples were randomly divided into two groups of 120 each and were labeled as group - L and group - LH. Group - LH specimens were further post heat-cured in an oven at 95°C for 25 min (Targis Power, Ivoclar, Vivadent, Schaan, Lichtenstein). All the specimens were then polished with 1200 grit silicon carbide grinding paper under running water to establish a uniformly flat surface and expose the glass fibres and the matrix between fibres. Next, the specimens were cleansed in deionized water in an ultrasonic bath (Quantrex 90; L&R Ultrasonics, USA) for 10 min and allowed to dry under ambient laboratory temperature (23°C ± 1°C) for 60 min.

The specimens in both the L and LH group were further grouped with 40 specimens each for treatment with ethanol concentrations of 99.9%, 70% and 40%. Within each concentration group the specimens were further sub-divided into four groups (n=10) for treatment with time interval of 15 s, 30 s, 60 s and 120 s respectively.

2.2. Experimental method.

Specimens were evaluated at the baseline and after being exposed to ethanol of various concentrations and treatment times. The surfaces of the prepared test specimens were subjected to the following analyses: the surface roughness (S_a), nano-mechanical properties (NMP) of the polymer matrix, chemical characterization, and surface visual analyses. Specimens were studied at the baseline and after being exposed to ethanol of various concentrations (99.9%, 70% and 40%) and treatment times (15 s, 30 s, 60 s and 120 s).

2.2.1. Surface roughness: A non-contact optical profilometer (Bruker, Contour GT, Tucson, AZ, USA) was used to assess the surface roughness (S_a) of the specimens. The profilometer is equipped with a Nanolens AFM module with a fully automated turret and X, Y and Z axis that are programmable providing a high resolution data. The high resolution data is converted into accurate 3D image software (simple vision 64). The measurements were taken randomly with five readings on each surface at different locations with a distance of 2 mm, and their mean value was calculated.

2.2.2. Nano-mechanical properties: The NMP (nano-hardness and modulus of elasticity) were measured using a nano-indenter (Bruker, Tucson, AZ, USA) equipped with a three sided Berkovich diamond indenter. The indenter was pressed on to the surface with preset loading and unloading values of 0.01 mN/s and 0.02 mN/s respectively with a maximum load of 20mN and a

resting period of 10 s. The test was performed under low noise conditions in a closed chamber and at controlled temperature of 23^{o} C.

2.2.3. Fourier Transform-Infrared (FTIR) spectroscopic analyses: The specimens from both the groups were subjected to surface characterization by FTIR (Vertex 80, Bruker, England, UK) in the wavenumber range of 750–1750 cm^{-1}. Attenuated Total Reflection (ATR) was employed for surface characterization by FTIR (Vertex 80, Bruker, England, UK) in the wavelength range of 600cm^{-}-4000cm^{-1}. Before the placement of the specimen the crystal was cleaned with isopropanol and dried with stream of nitrogen, making sure the specimen on the crystal makes a good contact. The specimens were subjected to ATR element made of Zinc-Selenide (Bruker, England, UK) wherein the infrared (IR) beam enters the ATR crystal at an angle of 45° which is totally reflected at the crystal to specimen interface. IR spectrum was plotted wavelength versus transmittance.

2.2.4. Scanning Electron Microscopy (SEM): SEM micrographs of the randomly selected specimens were taken for visual analysis (SEM, BOC EDWARDS, PV25MK, West Sussex, England, UK). The SEM devices were operated at voltage of 10 kV and a 250× magnification.

2.3. Statistical analysis

Statistical analysis of the data was performed using SPSS v. 20. Two ways AN0VA and Tukey's *post hoc* tests were applied. Regression analysis was performed for surface roughness and nano-mechanical properties at different concentrations of ethanol and at different time intervals. The significance level was determined to be $p \leq 0.05$.

3. Results.

Results for the S_a analysis for both light-cured (Group-L) and post heat-cured (Group-LH) FRC's showed that ethanol treatment had an influence to the surface roughness. Highest S_a (0.733 μm) was seen in the L group treated with 99.9 % ethanol for 120 s ($p < 0.05$). A statistically significant difference was seen for each concentrations of ethanol depending upon the treatment time ($p<0.05$). In the L group it was found that higher the concentration of ethanol and treatment time clearly increased the S_a, whereas in the LH group the S_a values varied less as shown in Table 1. Nano-mechanical properties for modulus of elasticity and nano-hardness were affected when treated with ethanol at varying concentrations and at different time period. Surface nano-hardness was higher for specimens which were light cured and additionally post heat cured than for specimens with light curing only. The highest surface nano-hardness was 1.91 GPa, measured for specimens of the LH-group treated with 99.9 % % ethanol for 120 s and the modulus of elasticity was the highest (22.90 GPa) for the group treated with 40 % ethanol for 120 s (Table 2). The representative nano-indentation curves are presented in Figure [1]. Figure [2] presents NMP plots during nano-indentation. A statistically significant difference was found for each concentration of ethanol depending upon the treatment time ($p<0.05$) (Table 2). Both the groups L and LH showed statistically significant changes at varying concentrations and time periods as shown in Tables 2 & 3.

Regression analysis demonstrated the correlation between the ethanol treatment time and surface roughness for the group-L and group-LH for 40% ethanol concentration (R^2=0.945, r=0.974, p<0.05) and (R^2=0.519, r=0.720, p<0.05), 70% ethanol concentration (R^2=0.981, r=0.990, p<0.05) and (R^2=0.906, r=0.952, p<0.05), and for 99.9% ethanol concentration (R^2=0.808, r=0.898, p<0.05) and (R^2=0.956, r=0.978, p<0.05) respectively as shown in Figure [3] & [4]. For ethanol treatment time and nano-hardness for the group-L and group-LH for 40% ethanol concentration (R^2=0.952, r=0.976, p<0.05) and (R^2=0.812, r=0.902, p<0.05), 70% ethanol concentration (R^2=0.732, r=0.856, p<0.05) and (R^2=0.842, r=0.918, p<0.05), and for 99.9% ethanol concentration (R^2=0.862, r=0.928, p<0.05) and (R^2=0.863, r=0.929, p<0.05) respectively as shown in Figure [5] & [6] and for ethanol treatment time and modulus of elasticity for the group-L and group-LH for 40% ethanol concentration (R^2=0.930, r=0.964, p<0.05) and (R^2=0.979, r=0.989, p<0.05), 70% ethanol concentration (R^2=0.542, r=0.732, p<0.05) and (R^2=0.861, r=0.928, p<0.05), and for 99.9% ethanol concentration (R^2=0.778, r=0.882, p<0.05) and (R^2=0.787, r=0.886, p<0.05) respectively as shown in Figures [7] &[8].

The FTIR analysis showed variation of peaks in the wavelength of 1650-1750 cm^{-1} for specimens of group-L. The peaks became higher by the prolonged ethanol exposure time as shown in Figure [9]. SEM images showed topographical changes caused by ethanol on the specimens on both the surface and cross section on comparison with the control group. Noticeable changes were seen and it varied based on the treatment time and different concentration groups, as shown in Figure [10].

4. Discussion.

The IPN resin matrix is used in dental FRCs for improving handling properties of fibre prepregs (pre-impregnated composite fibres with a thermoset polymer matrix material), and for enabling interfacial adhesion between the FRC and outermost resin composite layer. Synthesis of IPN would be either by a sequential IPN wherein a network is swollen and polymerized in the presence of other or both. The network precursors are synthesized simultaneously by independent, non-interfering route. Semi-IPN is formed when one of the two polymers is linear (non-crosslinked). Moreover mutual miscibility is an important consideration in their fabrication. Generally it has been seen that the polymers do not mix well each other, resulting in the phase separation of the final blend(Olabisi et al., 1979). In the semi IPN system of *bis*-GMA-TEGDMA-PMMA phase separation during the shelf life time of uncured prepegs, have been demonstrated to occur (Khan et al., 2018).

The organic matrix of dental FRC is formed by co-polymerization of dimethacrylate monomers in the presence of dissolved syndiotactic PMMA molecules (Ruyter and Oysaed, 1982). The ratio of PMMA and the cross-linked dimethacrylates varies in the FRC: there is more PMMA on the surface layer of FRC than in the inner parts. Now, the monomer composition in the polymer system exhibits features which determine their reactivity and mobility during the

formation of the IPN network, determining the degree of cure and density of the cross-linked polymer (Lovell et al., 1999). Even though *bis*-GMA is a highly reactive molecule, its phenolic groups impair the rotation about the bonds and the strong intermolecular interaction by the hydroxyl group renders it a very viscous material. Given this, the degree of conversion is never higher than 42% (Floyd and Dickens, 2006). TEGDMA or UEDMA monomers which are less viscous in nature are added in order to increase the DC and even in small quantities they have shown to improve the mechanical properties (Danso et al., 2018). On the other hand, at the same time increasing the polymerization shrinkage and water uptake (Kalachandra et al., 1993). The proportion ratio between the major monomers (*bis*-GMA and UDEMA) and minor monomers (TEGDMA) influenced the mechanical properties of the resin. The addition of minor monomers to the mixture decreased the viscosity, increased the DC, but increased the flexural strength up to an extent and beyond which the mechanical properties decreased (Asmussen and Peutzfeldt, 1998). Also, higher the level of *bis*-GMA in the matrix lower is the DC and also the mechanical properties of it is related to the chain extender in the *bis*-GMA molecule (Ogliari et al., 2008). Addition of PMMA to this *bis*-GMA-TEGDMA system also increases the viscosity, lowers rate of curing and lowers the modulus of elasticity of the polymer (Bouillaguet et al., 2006; Pastila et al., 2007).

Dissolution of the polymer primarily occurs by the diffusion of the solvent resulting in disentanglement of the polymeric chain. However, dissolution of the polymer is governed by whether it is poly or monodispersed and it also depends on its molecular weight (Manjkow, 1987). Diffusion of the solvent is also guided by the amount of non-crossed linked polymer backbones. It is noteworthy that PMMA is basically insoluble in water and ethanol alone at room temperature. However it is, soluble in ethanol-water mixture, (Brandrup.J, 1975) forming water

cages in PMMA and around the hydrophilic ethanol molecules at 40-50 vol-% and at 80 vol-% ethanol-water. In addition, hydrogen bonding is dominant around the ester moieties of the resin polymer which are being formed (Cowie et al., 1987) .

The polymer structure of IPN polymer incorporates several different kinds of intermolecular forces which hold the polymer chains together. The predominant ones are the covalent bonds of cross-links (namely phase of copolymer *bis*-GMA-TEGDMA), weaker hydrogen bonds and van der Waals bonds (a.k.a. London forces) between the polymer chains of the non-cross-linked PMMA chains. By and large, in the dissolution process there are two stages: polymer swelling and the dissolution stage itself. The exposure time of 120 s in maximum could have started the swelling stage and after evaporation of ethanol, the polymer chains of PMMA of the swelled layer are oriented second time and form a solid polymer layer. Polymer chains of the reorganized PMMA on the surface layer of the FRC may have even formed crystallized regions by which the surface hardness and modulus of elasticity were increased. Had the ethanol exposure time considerably longer, the actual dissolving stage would have occurred large. This has been reported for PMMA based denture base polymers after being dissolved by ethanol for 30 days (Regis et al., 2009).

In fact, one of the crystallization techniques is solvent induced crystallization (Andjelić and Scogna, 2015). In the most cases the solvent uptake causing swelling of the polymer surface is non-Fickian due to multiple polymer chain segmental relaxations. After evaporation of the solvent and solidification, at least some degree of crystallization may have occurred which has hardened the surface (Aly, 2015.). Tacticity of the PMMA of has been shown to relate to the crystallization supporting the findings for the suggested crystallization with syndiotactoc PMMA (John et al., 1989). Nanometer scale surface hardening after a short term exposure to ethanol has

been demonstrated also in our previous studies (Basavarajappa et al., 2017). Further studies are needed to confirm and investigate the possible crystallization of the PMMA after being exposed with ethanol.

When the cross-linked part of the polymer matrix is considered from the perspective of solvent dissolution, it is known that the dental dimethacrylate resin composite systems reacts with solvents complex and they are obviously related to the chemical structure of the resin (Ferracane, 2006). That said, it has been shown that different components of the resin matrix such as *bis*-GMA, UEDMA, TEGDMA, have differed in their solubility percentile at different concentrations of ethanol and water (Sideridou and Karabela, 2011). Basically, a well polymerized *bis*-GMA based resin composite is relatively resistant to solvent effect by ethanol (Asmussen, 1984).

Different vibrations of the functional groups in the molecules give rise to different intensity of the peaks in the IR spectra. The intensity of the peak is governed by various factors such as absorbance, absorption, path-length, humidity and concentration and the width of the band determined by the chemical environment determined by the intermolecular interactions. These components of the resin matrix are chemically characterized by various carbon to carbon (C-C, C=C), carbon to hydrogen (C-H), carbon to oxygen (C-O or C=O or C-O-C), bonds. The ATR-FTIR spectroscopy has shown that C-H bonds are seen in the wavelengths between 850-920 cm^{-1} and 1141-1271 cm^{-1} for the C-O and C-O-C group, and C=O at 1650-1750 cm^{-1} and also within the aromatic bands (Moraes et al., 2008). In the current study we have found that the peaks for carbonyl group (C=O) at the wavelength range of 1650-1750 cm^{-1} became higher (more intensive) if the surface was exposed to ethanol. This may relate to possible crystallization of the outermost layer of the polymer matrix and enrichment of linear polymer to the surface

along with better detection of the methacrylate groups of the polymer network resulting by the elimination of the polishing debris via ethanol.

In the current study we also found that the surface roughness (S_a) was influenced by ethanol at varying concentrations and treatment time. This was likely related to the swelling and resolidification of the polymer surface between the glass fibers which were not affected by ethanol. It is also possible that some of residual monomers may have leached from the polymer matrix and had a minor effect on the dimensions of the polymer matrix between the fibres (Pedreira et al., 2009; Polydorou et al., 2009).

From the practical point of view the current results have an impact for better understanding of effects of commonly used ethanol containing dental primers, disinfectants and mouth rinses to the IPN polymers and polymer matrices of resin composites. From the material research and development perspective, the results of this study may open new ways of modify the polymer surface crystallization.

Conclusion

This laboratory study suggests that both light-cured and light cured with heat post-cured FRCs having an IPN polymer matrix was influenced by the exposure of ethanol. Some clear influence was found as changes of the surface roughness and nano-mechanical properties. A short term ethanol exposure increased the surface nano-hardness and modulus of elasticity

Conflict of interest: Author PV consults Stick Tech – Member of GC Group in R&D and training.

Acknowledgement:

The authors extend their appreciation to the International Scientific Partnership Program ISPP at King Saud University for funding this research work through ISPP#0088. Study is also part of BioCity Turku Biomaterials and Medical Device Research Program (www.biomaterials.utu.fi).

References.

Abate, P.F., Rodriguez, V.I., Macchi, R.L., 2000. Evaporation of solvent in one-bottle adhesives. J.Dent. 28, 437-440.

Aly, A.A., 2015. Heat treatment of polymers: A review. Int. J. Mater. Chem. Phys. 1, 132-140.

Andjelić, S., Scogna, R.C., 2015. Polymer crystallization rate challenges: The art of chemistry and processing. J.Appl. Polym. Sci. 132.

Asmussen, E., 1984. Softening of BISGMA-based polymers by ethanol and by organic acids of plaque. Scand. J. Dent. Res. 92, 257-261.

Asmussen, E., Peutzfeldt, A., 1998. Influence of UEDMA BisGMA and TEGDMA on selected mechanical properties of experimental resin composites. Dent Mater. 14, 51-56.

Basavarajappa, S., Al-Kheraif, A.A.A., Alhijji, S.M., Matinlinna, J.P., Vallittu, P.K., 2017. Effect of ethanol treatment on mechanical properties of heat-polymerized polymethyl methacrylate denture base polymer. Dent.Mater. J. 36, 834-841.

Basavarajappa, S., Al-Kheraif, A.A.A., ElSharawy, M., Vallittu, P.K., 2016. Effect of solvent/disinfectant ethanol on the micro-surface structure and properties of multiphase denture base polymers. J.Mech.Behav.Biomed.Mater. 54, 1-7.

Le Bell, A.-M.L., Lassila, L.V.J., Kangasniemi, I., Vallittu, P.K., 2005. Bonding of fibre-reinforced composite post to root canal dentin. J. Dent. 33, 533-539.

Bouillaguet, S., Schütt, A., Alander, P., Schwaller, P., Buerki, G., Michler, J., Cattani-Lorente, M., Vallittu, P.K., Krejci, I., 2006. Hydrothermal and mechanical stresses degrade fiber–matrix interfacial bond strength in dental fiber-reinforced composites. J. Biomed.l Mater. Res. B. 76B, 98-105.

Bowen, R.L., 1963. Properties of a silica-reinforced polymer for dental restorations. J.Am. Dent.Assoc. 66, 57-64.

Brandrup.J, 1975. Polymer Handbook., Second ed. John Wiley and Sons, New York. pp 340-354.

Cowie, J.M.G., Mohsin, M.A., McEwen, I.J., 1987. Alcohol-water cosolvent systems for poly(methyl methacrylate). Polymer. 28, 1569-1572.

Danso, R., Hoedebecke, B., Whang, K., Sarrami, S., Johnston, A., Flipse, S., Wong, N., Rawls, H.R., 2018. Development of an oxirane/acrylate interpenetrating polymer network (IPN) resin system. Dent.Mater. 34,1459-1465.

Dyer, S.R., Lassila, L.V.J., Jokinen, M., Vallittu, P.K., 2004. Effect of fiber position and orientation on fracture load of fiber-reinforced composite. Dent.Mater. 20,947-955.

Ekambaram, M., Yiu, C.K.Y., Matinlinna, J.P., 2015. An overview of solvents in resin–dentin bonding. Int.J.Adhes.Adhes. 57, 22-33.

Ferracane, J.L., 2006. Hygroscopic and hydrolytic effects in dental polymer networks. Dent. Mater. 22, 211-222.

Floyd, C.J.E., Dickens, S.H., 2006. Network structure of Bis-GMA- and UDMA-based resin systems. Dent.Mater.22,1143-1149.

Fontes, S.T., Lima, G.S., Ogliari, F.A., Piva, E., Moraes, R.R., 2012. Hybridization morphology and dentin bond stability of self-etch primers with different ethanol/water ratios. Odontology. 100, 181-186.

Garoushi, S., Vallittu, P.K., Watts, D.C., Lassila, L.V.J., 2008. Polymerization shrinkage of experimental short glass fiber-reinforced composite with semi-inter penetrating polymer network matrix. Dent.Mater.24,211-215.

John, E., Jeon, S.H., Ree, T., 1989. Influence of tacticity of poly(methyl methacrylate) on the morphology and crystallization of poly(ethylene oxide) in the binary polymer blends. J. Polym. Sci. C: Polymer Letters 27, 9-19.

Kalachandra, S., Taylor, D.F., DePorter, C.D., Grubbs, H.J., McGrath, J.E., 1993. Polymeric materials for composite matrices in biological environments. Polymers. 34, 778-782.

Kambour, R.P., 1973. A review of crazing and fracture in thermoplastics. Polym.Rev. 7, 1-154.

Khan, A.A., Al-Kheraif, A.A., Al-Shehri, A.M., Säilynoja, E., Vallittu, P.K., 2018. Polymer matrix of fiber-reinforced composites: Changes in the semi-interpenetrating polymer network during the shelf life. J.Mech.Behav.Biomed.Mater. 78, 414-419.

Klempner, D., Frisch, H.L., Frisch, K.C., 1970. Topologically interpenetrating elastomeric networks. J.Polym.Sci., Part A-2: Polym.Phy. 8, 921-935.

Kolbeck, C., Rosentritt, M., Behr, M., Lang, R., Handel, G., 2002. In vitro examination of the fracture strength of 3 different fiber-reinforced composite and 1 all-ceramic posterior inlay fixed partial denture systems. J.Prosthodont. 11, 248-253.

Ladizesky, N.H., Cheng, Y.Y., Chow, T.W., Ward, I.M., 1993. Acrylic resin reinforced with chopped high performance polyethylene fiber-properties and denture construction. Dent.Mater. 9, 128-135.

Lastumäki, T.M., Kallio, T.T., Vallittu, P.K., 2002. The bond strength of light-curing composite resin to finally polymerized and aged glass fiber-reinforced composite substrate. Biomaterials. 23, 4533-4539.

Lovell, L.G., Stansbury, J.W., Syrpes, D.C., Bowman, C.N., 1999. Effects of Composition and Reactivity on the Reaction Kinetics of Dimethacrylate/Dimethacrylate Copolymerizations. Macromolecules. 32, 3913-3921.

Manjkow, J., Papanu, J.S., Hess, D.W., Soane, D.S/, Bell, A.T., 1987. Influence of processing and molecular parameters on the dissolution rate of poly-(methyl mathacrylate) thin films. J. Electrochem.Soc. 134, 2003-2007.

Matinlinna, J.P., Lassila, L.V.J., Özcan, M., Yli-Urpo, A., Vallittu, P,K., 2004. An Introduction to silanes and their applications in dentistry. Int. J. Prosthodont.17, 155-164.

Matinlinna, J.P., Lung, C.Y.K., Tsoi, J.K.H., 2018. Silane adhesion mechanism in dental applications and surface treatments: A review. Dent. Mater.34, 13-28.

McLeish, T.C.B., Plummer, C.J.G., Donald, A.M., 1989. Crazing by disentanglement: non-diffusive reptation. Polymer. 30, 1651-1655.

Miettinen, V.M., Vallittu, P.K., 1997. Water sorption and solubility of glass fiber-reinforced denture polymethyl methacrylate resin. J. Prosthet. Dent.77, 531-534.

Moraes, L.G.P., Rocha, R.S.F., Menegazzo, L.M., de AraÚjo, E.B., Yukimitu, K., Moraes, J.C.S., 2008. Infrared spectroscopy: A tool for determination of the degree of conversion in dental composites. J.Appl.Oral.Sci. 16, 145-149.

Myung, D., Waters, D., Wiseman, M., Duhamel, P.-E., Noolandi, J., Ta, C.N., Frank, C.W., 2008. Progress in the development of interpenetrating polymer network hydrogels. Polym.Adv. Technol. 19, 647-657.

Nowers, J.R., Narasimhan, B., 2006. The effect of interpenetrating polymer network formation on polymerization kinetics in an epoxy-acrylate system. Polymer. 47, 1108-1118.

Ogliari, F.A., Ely, C., Zanchi, C.H., Fortes, C.B.B., Samuel, S.M.W., Demarco, F.F., Petzhold, C.L., Piva, E., 2008. Influence of chain extender length of aromatic dimethacrylates on polymer network development. Dent.Mater. 24, 165-171.

Olabisi, O., Robeson, L.M., Shaw, M.T., 1979.Methods for Determining Polymer-Polymer Miscibility, Polymer–Polymer Miscibility.Academic Press, pp. 117-193.

Pastila, P., Lassila, L.V., Jokinen, M., Vuorinen, J., Vallittu, P.K., Mantyla, T., 2007. Effect of short-term water storage on the elastic properties of some dental restorative materials-A resonant ultrasound spectroscopy study. Dent. Mater. 23, 878-884.

Pedreira, A.P.R.V., Pegoraro, L.F., de Góes, M.F., Pegoraro, T.A., Carvalho, R.M., 2009. Microhardness of resin cements in the intraradicular environment: Effects of water storage and softening treament. Dent.Mater. 25, 868-876.

Polydorou, O., König, A., Hellwig, E., Kümmerer, K., 2009. Long-term release of monomers from modern dental-composite materials. Eur.J.Oral.Sci. 117, 68-75.

Regis, R.R., Soriani, N.C., Azevedo, A.M., Silva-Lovato, C.H., Oliveira Paranhos, H.F., De Souza, R.F., 2009. Effects of Ethanol on the Surface and Bulk Properties of a Microwave-Processed PMMA Denture Base Resin. J. Prosthodont. 18, 489-495.

Reis, A.F., Oliveira, M.T., Giannini, M., De Goes, M.F., Rueggeberg, F.A., 2003. The effect of organic solvents on one-bottle adhesives' bond strength to enamel and dentin. Oper. Dent. 28, 700-706.

Ruyter, I.E., Oysaed, H., 1982. Conversion in denture base polymers. J. Biomed. Mater. Res. 16, 741-754.

Sideridou, I.D., Karabela, M.M., 2011. Sorption of water, ethanol or ethanol/water solutions by light-cured dental dimethacrylate resins. Dent. Mater. 27, 1003-1010.

Sperling, L.H., 1985. Recent advances in interpenetrating polymer networks. Polym.Eng.&Sci. 25, 517-520.

Sperling, L.H., 1994. Interpenetrating Polymer Networks: An Overview, Interpenetrating Polymer Networks. J.Am.Chem.Soc. 239, 3-38.

Sweeney, W.T., Caul, H.J., 1940. Denture Rubber: Composition, Properties and a Specification. J.Am.Dent.Assoc. 27, 1446-1458.

Vallittu, P.K., 1994. Acrylic resin-fiber composite—part II: The effect of polymerization shrinkage of polymethyl methacrylate applied to fiber roving on transverse strength. J. Prosthet. Dent. 71, 613-617.

Vallittu, P.K., 1995. Impregnation of glass fibres with polymethylmethacrylate using a powder-coating method. Appl. Compos. Mater. 2, 51-58.

Vallittu, P.K., 1996. A Review of Fiber-Reinforced Denture Base Resins. J.Prosthodont. 5, 270-276.

Vallittu, P.K., 2009. Interpenetrating Polymer Networks (IPNs) in Dental Polymers and Composites. J.Adhes.Sci.Technol. 23, 961-972.

Vallittu, P.K., Lassila, V.P., Lappalainen, R., 1994. Acrylic resin-fiber composite—part I: The effect of fiber concentration on fracture resistance. J.Prosthet.Dent. 71, 607-612.

Wolff, D., Geiger, S., Ding, P., Staehle, H.J., Frese, C., 2012. Analysis of the interdiffusion of resin monomers into pre-polymerized fiber-reinforced composites. Dent. Mater. 28, 541-547.

Yiu, C.K.Y., Pashley, E.L., Hiraishi, N., King, N.M., Goracci, C., Ferrari, M., Carvalho, R.M., Pashley, D.H., Tay, F.R., 2005. Solvent and water retention in dental adhesive blends after evaporation. Biomaterials. 26, 6863-6872.

Table-1: Statistical results of surface roughness (S_a) in μm of light-cured (L) and light-cured with additional post-curing with heat (LH)-FRC.

L-Group		Baseline	15 s	30 s	60s	120 s
99.9% Ethanol	Mean	0.325^{a}	0.535^{b}	0.540^{b}	0.624^{c}	0.733^{d}
	S.D	0.010	0.009	0.040	0.023	0.062
70% Ethanol	Mean	0.226^{a}	0.225^{a}	0.253^{b}	0.275^{b}	0.328^{b}
	S.D	0.017	0.013	0.020	0.011	0.009
40% Ethanol	Mean	0.158^{a}	0.157^{a}	0.158^{a}	0.203^{b}	0.255^{c}
	S.D	0.012	0.009	0.022	0.021	0.023
LH-Group						

99.9% Ethanol	Mean	0.142[a]	0.145[a]	0.173[b]	0.189[b]	0.222[d]
	S.D	0.017	0.005	0.004	0.014	0.013
70% Ethanol	Mean	0.140[a]	0.146[a]	0.152[a]	0.189[b]	0.202[b]
	S.D	0.004	0.004	0.013	0.022	0.005
40% Ethanol	Mean	0.134[a]	0.143[a]	0.159[a]	0.160[a]	0.159[a]
	S.D	0.012	0.009	0.022	0.021	0.023

Different superscript small letters in the same row indicate statistically significant at $P<0.05$.

Table 2: Statistical results of surface nanohardness (GPa) of polymer matrix of light-cured (L) and light-cured with additional post-curing wit heat (LH)-FRC.

L-Group		Baseline	15 s	30 s	60s	120 s
99.9% Ethanol	Mean	0.108[a]	0.424[b]	0.655[b]	1.139[c]	1.296[c]
	S.D	0.066	0.009	0.040	0.023	0.062
70% Ethanol	Mean	0.108[a]	0.649[b]	0.835[b]	1.245[c]	1.292[c]
	S.D	0.066	0.056	0.095	0.076	0.096
40% Ethanol	Mean	0.108[a]	0.369[b]	0.517[b]	1.021[c]	1.383[d]
	S.D	0.066	0.093	0.069	0.090	0.099

LH-Group						
99.9% Ethanol	Mean	0.301[a]	0.586[b]	1.081[c]	1.669[d]	1.908[e]
	S.D	0.051	0.091	0.086	0.047	0.060
70% Ethanol	Mean	0.301[a]	0.647[b]	1.065[c]	1.734[d]	1.895[d]
	S.D	0.051	0.084	0.096	0.067	0.066
40% Ethanol	Mean	0.301[a]	0.727[b]	1.149[c]	1.189[c]	1.579[d]
	S.D	0.051	0.094	0.091	0.083	0.068

Different superscript small letters in the same row indicate statistically significant at $P<0.05$.

Table 3: Statistical results of modulus of elasticity (GPa) of polymer matrix of light-cured (L) and light-cured with additional post-curing with heat (LH)-FRC.

L-Group		Baseline	15 s	30 s	60s	120 s
99.9% Ethanol	Mean	4.856[a]	8.648[b]	9.894[b]	14.329[c]	14.663[c]
	S.D	0.171	0.491	0.638	0.438	0.654
70% Ethanol	Mean	4.856[a]	11.855[b]	15.754[c]	15.797[c]	16.863[c]
	S.D	0.171	0.377	0.367	0.222	0.316
40% Ethanol	Mean	4.856[a]	8.687[b]	9.893[b]	12.946[c]	16.568[d]
	S.D	0.171	0.346	0.431	0.451	0.445
LH-Group						

99.9% Ethanol	Mean	8.882^{a}	12.592^{b}	16.006^{c}	19.516^{d}	20.533^{d}
	S.D	0.592	0.197	0.054	0.242	0.111
70% Ethanol	Mean	8.882^{a}	11.090^{b}	12.615^{b}	19.937^{c}	21.217^{c}
	S.D	0.592	0.248	0.432	0.542	0.139
40% Ethanol	Mean	8.882^{a}	11.371^{b}	13.059^{b}	17.811^{c}	22.798^{d}
	S.D	0.592	0.572	0.658	0.603	0.104

Different superscript small letters in the same row indicate statistically significant at $P<0.05$.

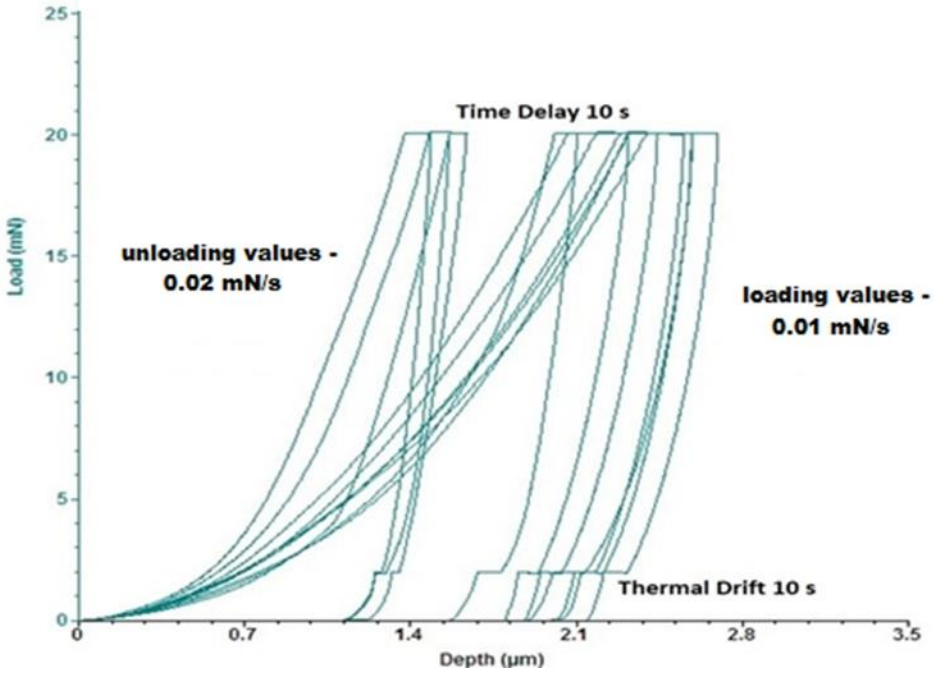

Figure-1: Graphs illustrating the loading and unloading of the force and plotted values for nano-hardness and the Young's modulus of elasticity of Light-cured group with 99.9 % ethanol for 120 s.

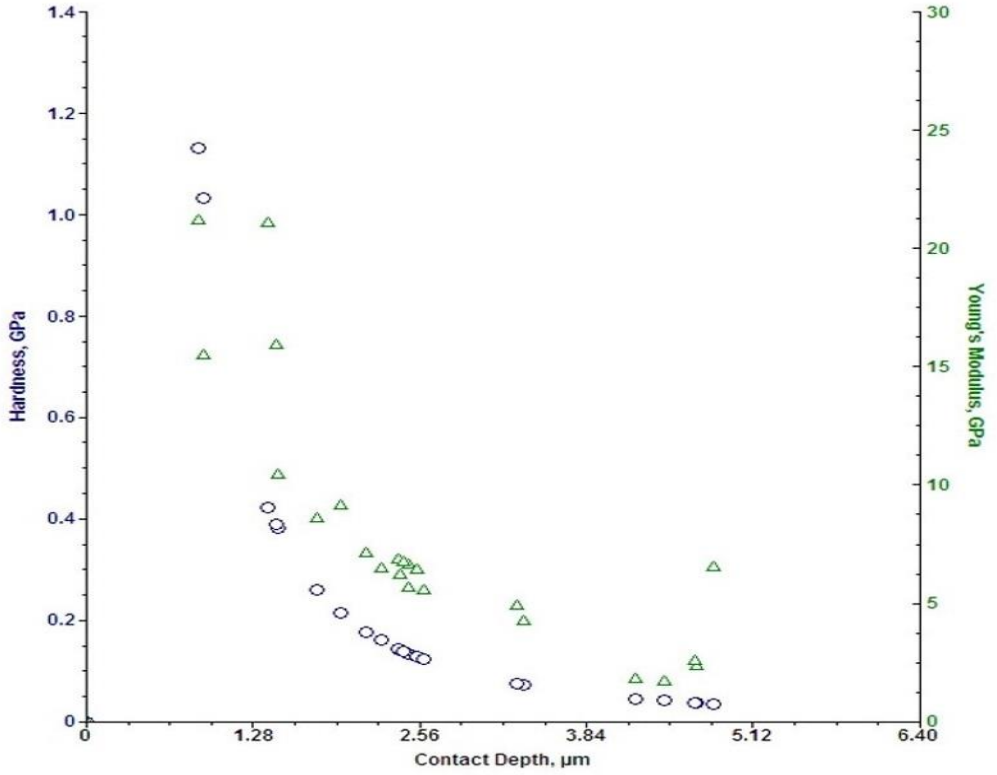

Figure-2: Values of the contact depth (µm) plotted against surface nanohardness (GPa) (y-axis on the left) and elastic modulus (GPa) (y-axis on the right) of Light-cured group with 99.9 % ethanol for 120 s.

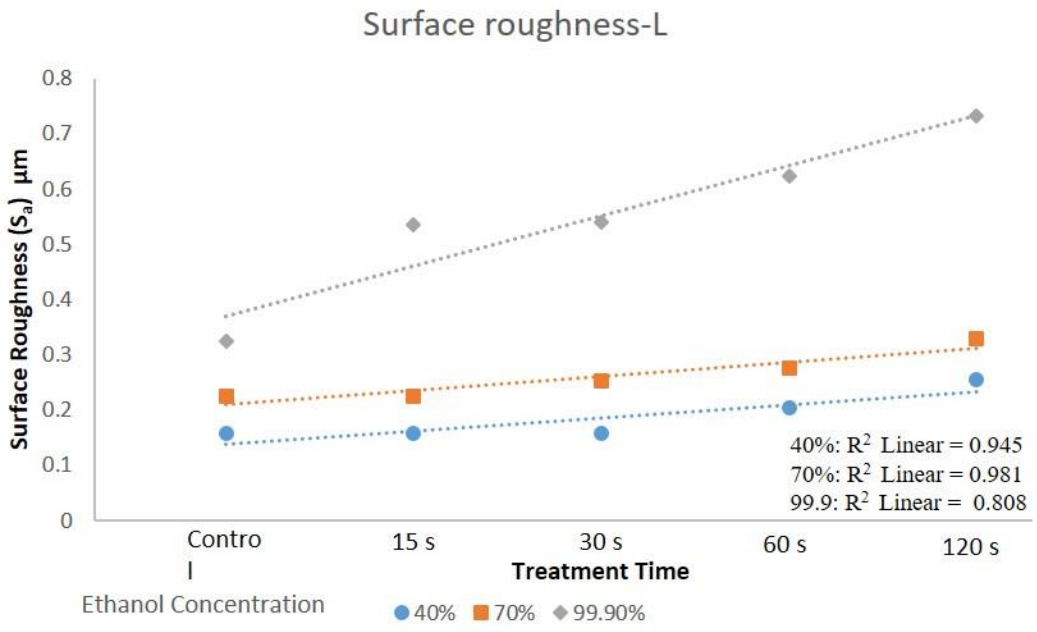

Figure-3: Regression analysis correlation between ethanol treatment time and surface roughness for light-cured specimens (Group-L).

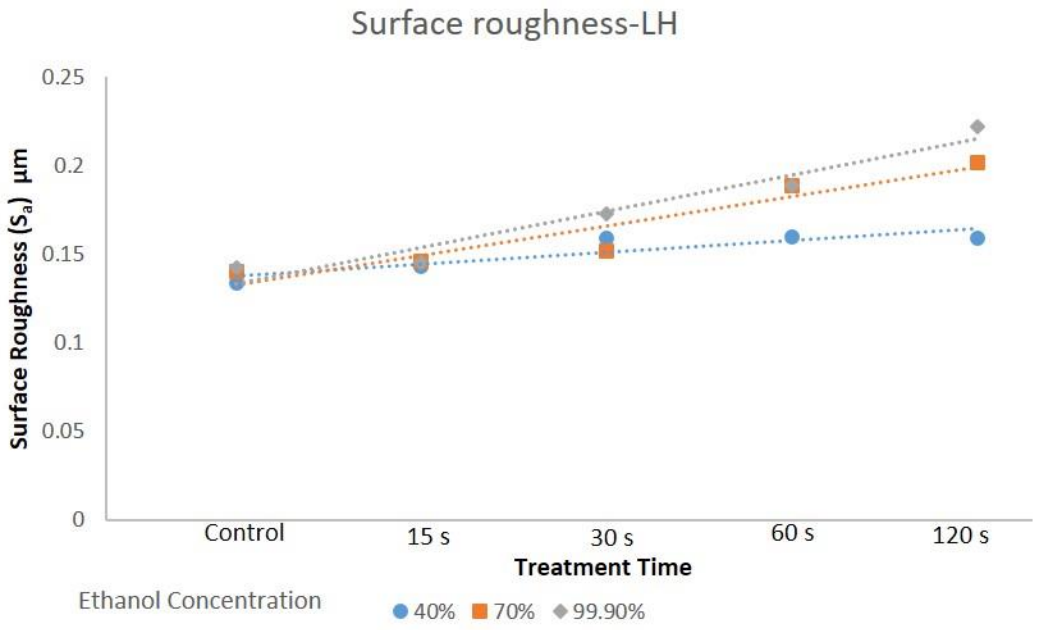

Figure-4: Regression analysis correlation between ethanol treatment time and surface roughness for light and heat-cured specimens (Group-LH).

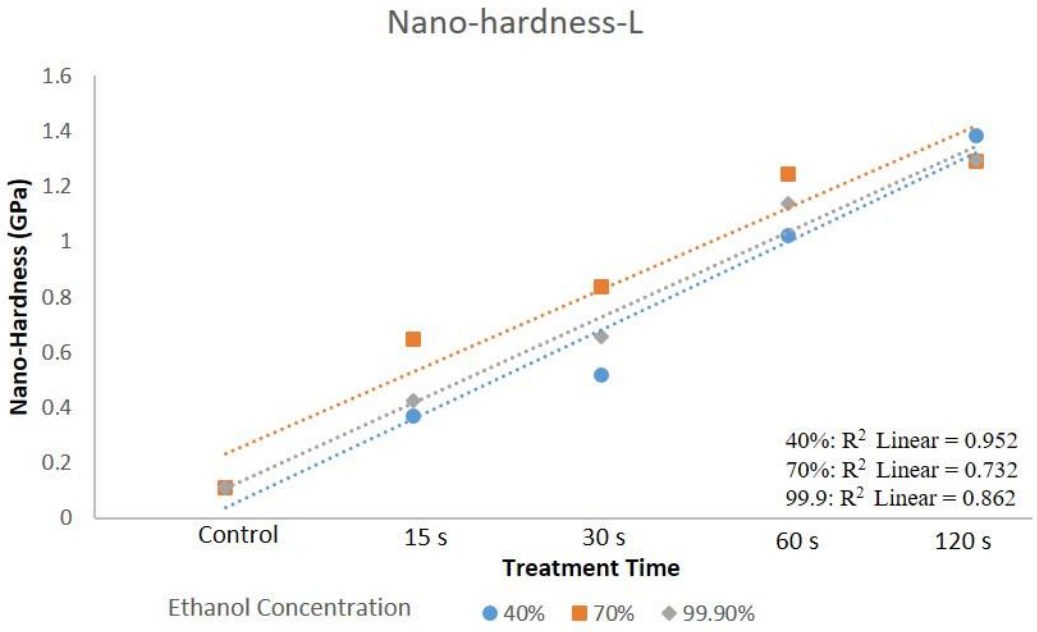

Figure-5: Regression analysis correlation between ethanol treatment time and nano-hardness for light-cured specimens (Group-L).

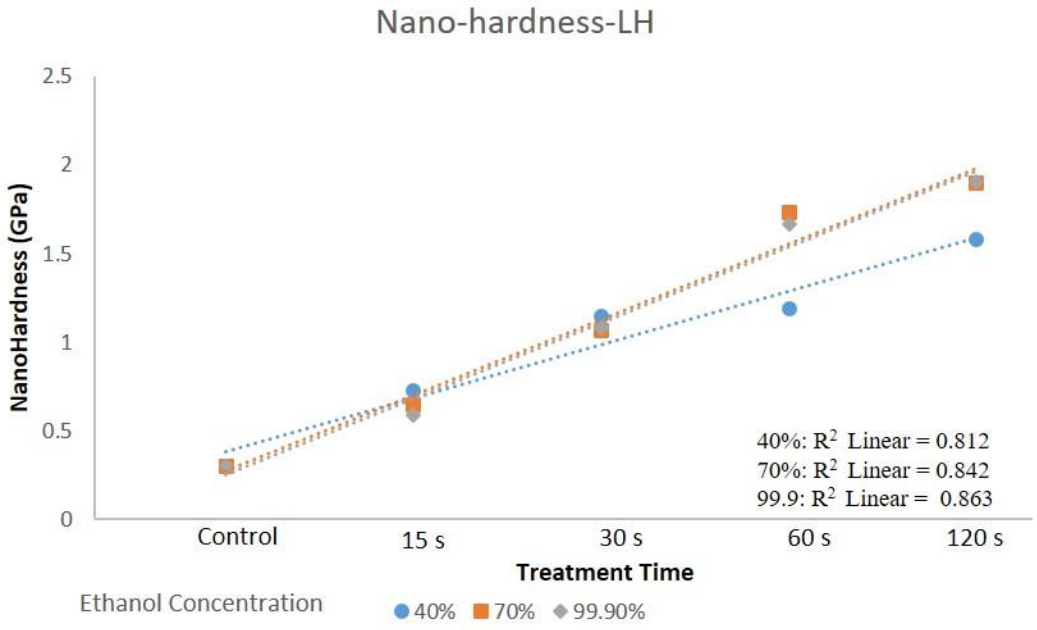

Figure-6: Regression analysis correlation between ethanol treatment time and nano-hardness for light and heat-cured specimens (Group-LH).

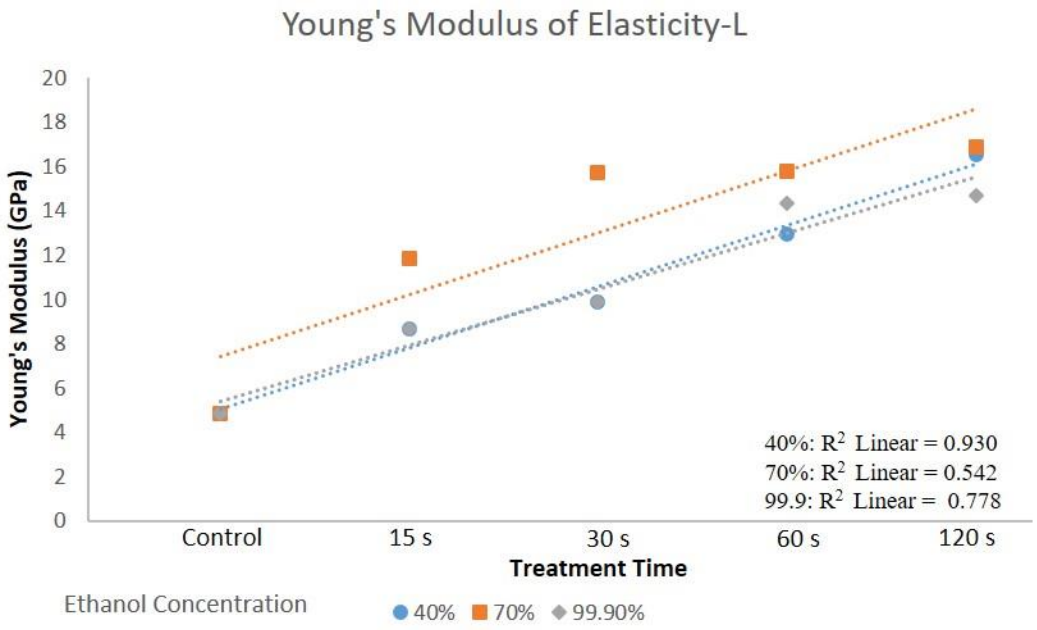

Figure-7: Regression analysis correlation between ethanol treatment time and modulus of elasticity for light-cured specimens (Group-L).

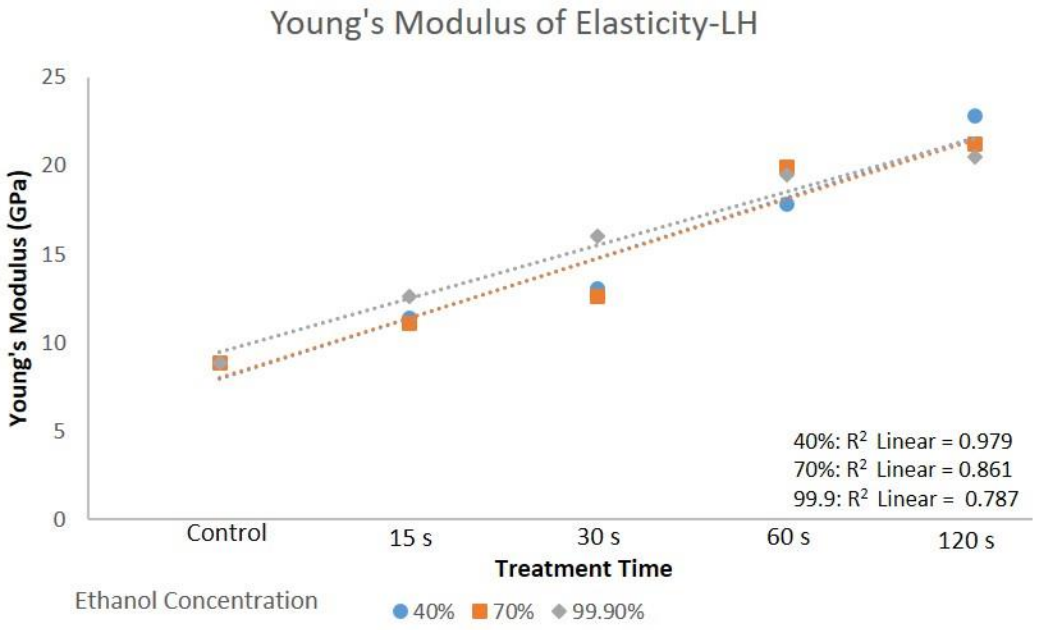

Figure-8: Regression analysis correlation between ethanol treatment time and modulus of elasticity for light and heat-cured specimens (Group-LH).

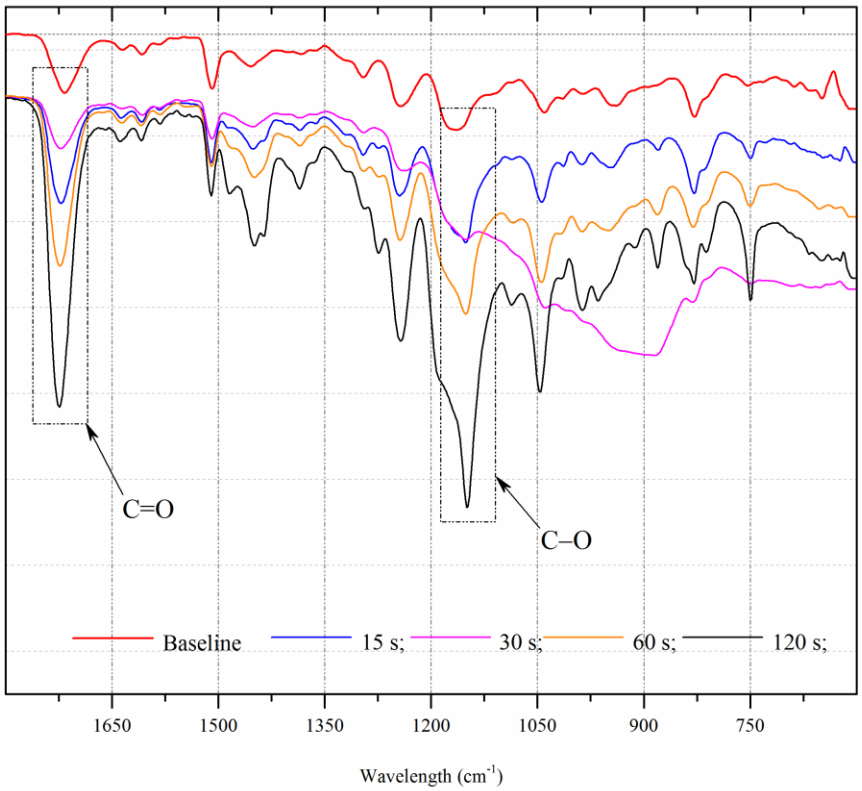

Figure 9: FTIR spectrum for specimens of light-cured specimens (Group-L) exposed by 99.9 % ethanol for 0 (Baseline), 15, 30, 60 and 120 s. Arrows are depicting the peaks of carbonyl groups(C=O) and aromatic groups (C-O).

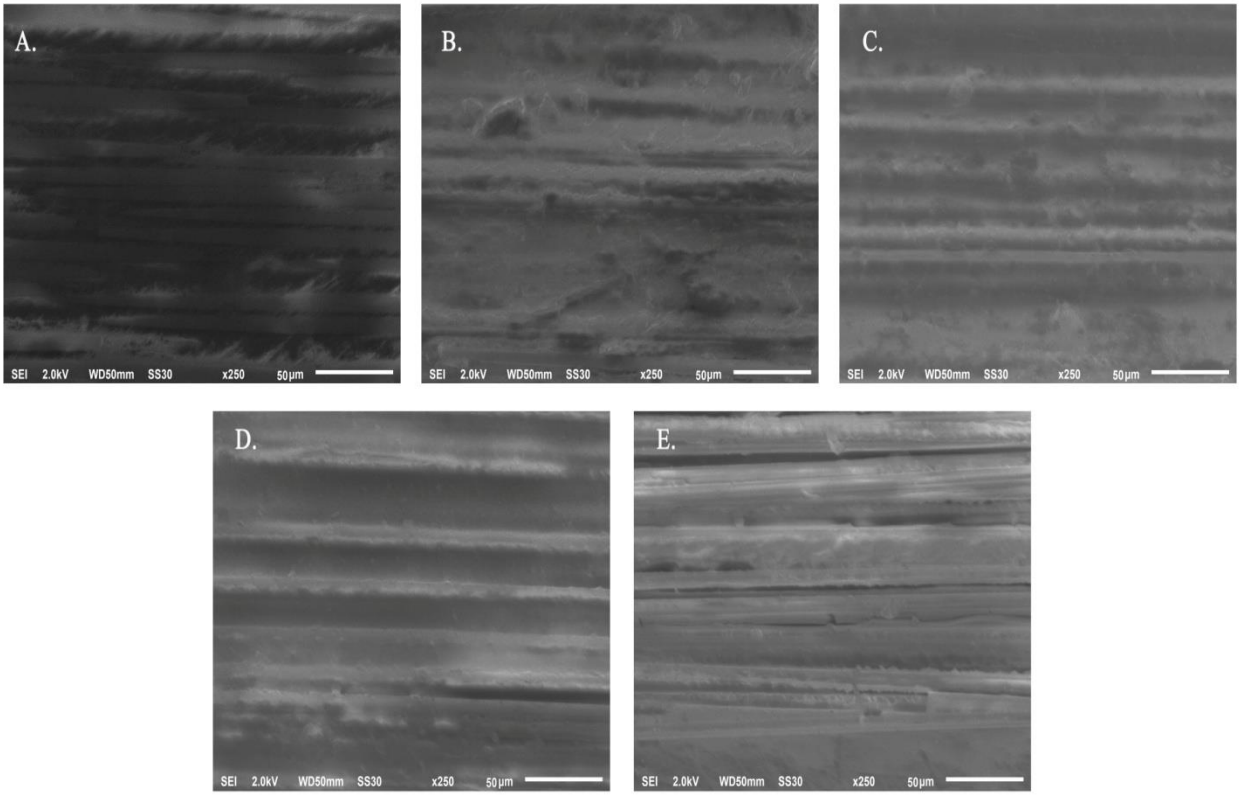

Figure-10: SEM images on the surface of light-cured specimens (Group-L) treated with 99.9% ethanol concentration for baseline (A) and various lengths of time (B, C, D and E for 15 s, 30 s, 60 s and 120 s respectively). Original magnification of 250 x, bar = 50 μm.